Am J Physiol Renal Physiol 284: F852–F862, 2003.
First published December 3, 2002; 10.1152/ajprenal.00210.2002.

ADF/cofilin mediates actin cytoskeletal alterations in LLC-PK cells during ATP depletion

Sharon L. Ashworth,[1] Erica L. Southgate,[1] Ruben M. Sandoval,[1] Peter J. Meberg,[2] James R. Bamburg,[3] and Bruce A. Molitoris[1]

[1]*Division of Nephrology, Department of Medicine, Indiana University, and Roudebush Veterans Affairs Medical Center, Indianapolis, Indiana 46202-5116;* [2]*Department of Biology, University of North Dakota, Grand Forks, North Dakota 58201; and* [3]*Department of Biochemistry and Molecular Biology, Colorado State University, Fort Collins, Colorado 80523-1870*

Submitted 5 June 2002; accepted in final form 22 November 2002

Ashworth, Sharon L., Erica L. Southgate, Ruben M. Sandoval, Peter J. Meberg, James R. Bamburg, and Bruce A. Molitoris. ADF/cofilin mediates actin cytoskeletal alterations in LLC-PK cells during ATP depletion. *Am J Physiol Renal Physiol* 284: F852–F862, 2003. First published December 3, 2002; 10.1152/ajprenal.00210.2002.—Ischemic injury induces actin cytoskeleton disruption and aggregation, but mechanisms affecting these changes remain unclear. To determine the role of actin-depolymerizing factor (ADF)/cofilin participation in ischemic-induced actin cytoskeletal breakdown, we utilized porcine kidney cultured cells, LLC-$PK_{A4.8}$, and adenovirus containing wild-type (wt), constitutively active, and inactive *Xenopus* ADF/cofilin linked to green fluorescence protein [XAC(wt)-GFP] in an ATP depletion model. High adenoviral infectivity (70%) in LLC-$PK_{A4.8}$ cells resulted in linearly increasing XAC(wt)-GFP and phosphorylated (p)XAC(wt)-GFP (inactive) expression. ATP depletion rapidly induced dephosphorylation, and, therefore, activation, of endogenous pcofilin as well as pXAC(wt)-GFP in conjunction with the formation of fluorescent XAC(wt)-GFP/actin aggregates and rods. No significant actin cytoskeletal alterations occurred with short-term ATP depletion of LLC-$PK_{A4.8}$ cells expressing GFP or the constitutively inactive mutant XAC(S3E)-GFP, but cells expressing the constitutively active mutant demonstrated nearly instantaneous actin disruption with aggregate and rod formation. Confocal image three-dimensional volume reconstructions of normal and ATP-depleted LLC-$PK_{A4.8}$ cells demonstrated that 25 min of ATP depletion induced a rapid increase in XAC(wt)-GFP apical and basal signal in addition to XAC-GFP/actin aggregate formation. These data demonstrate XAC(wt)-GFP participates in ischemia-induced actin cytoskeletal alterations and determines the rate and extent of these ATP depletion-induced cellular alterations.

ischemia; microvilli; actin-depolymerizing factor; XAC-GFP

ISCHEMIA-INDUCED CELL INJURY of polarized proximal tubule cells results in severe biochemical, physiological, and morphological alterations (13, 20, 33). The extent of cellular injury is affected by the length and severity of the ischemic insult (14). Cellular changes in surface membrane polarity, junctional complexes, and the actin cytoskeleton are among the earliest observed alterations (14, 22, 23, 30). Within 5 min of ischemic injury induction, renal proximal tubule actin cytoskeletal alterations begin with the apical microvilli showing signs of degeneration (13, 14, 20, 21). With increasing duration of ischemic injury, the apical microvilli suffer further damage with complete disintegration of their microfilament cores and overlying plasma membranes. Microvillar membranes fuse or coalesce to form enlarged structures, and membrane vesicles or blebs also form (28). These abnormal microvillar vesicles are internalized within the proximal tubule cytoplasm or lost into the proximal tubule lumen. The cellular mechanisms responsible for the microfilament alterations are not known. In addition to microvillar F-actin rearrangement in proximal tubule cells in response to ischemia, cytosolic F-actin redistributes with formation of F-actin aggregates (12, 15, 24).

Our previous in vivo data are consistent with a role for the actin-depolymerizing factor (ADF)/cofilin family of proteins in proximal tubule apical microvillar breakdown (3, 29). The ADF/cofilin family of proteins is necessary for eukaryotic cell survival, although the number and type of isoforms may vary between cell types (32). These proteins are among the most important cellular regulators of actin filament dynamics. They bind F-actin in a pH-dependent manner and have been shown to mediate F-actin severing and depolymerization (5). Under physiological conditions, ADF has a diffuse cytoplasmic distribution with little or no localization in the apical region of proximal tubule cells, but with induction of ischemia, this distribution pattern changes dramatically. Within 15 min of ischemia, the phosphorylated or inactive form of the ADF protein (25) is rapidly dephosphorylated (29) and translocated from the cytoplasm into the terminal web and apical microvilli (3). Both actin and ADF have been localized to luminal membrane vesicles that have been lost from the apical surface during ischemic injury. Although these data are consistent with participation of ADF/cofilin in destruction of the F-actin core of

Address for reprint requests and other correspondence: B. Molitoris, Division of Nephrology, Indiana Univ. School of Medicine, 1120 South Dr., FH 115, Indianapolis, IN 46202-5116 (E-mail: bmolitor@iupui.edu).

The costs of publication of this article were defrayed in part by the payment of page charges. The article must therefore be hereby marked "*advertisement*" in accordance with 18 U.S.C. Section 1734 solely to indicate this fact.

microvilli in response to ischemic injury of proximal tubule cells, direct proof for this role is lacking.

Therefore, the present studies were undertaken to directly evaluate the role ADF plays in F-actin destruction and reorganization during ischemic cell injury. To accomplish this goal, we utilized the proximal tubule cell line LLC-PK because several studies have demonstrated F-actin reorganization observed in rat proximal tubule cells in response to ischemic insult can be mimicked in LLC-PK cells by inducing ATP depletion through treatment with antimycin A in substrate-depleted medium (4, 10, 15, 24). Recently, adenoviral constructs containing cDNAs of the wild-type (wt) ADF/cofilin isoform, *Xenopus* ADF/cofilin, XAC(wt)-green fluorescent protein (GFP), the constitutively active mutant, XAC(S3A)-GFP, and the inactive mutant, XAC(S3E)-GFP, have become available (1, 18) and allowed for expression of these proteins in LLC-PK cells. These unique tools have been successfully used for expression of the wild-type ADF/cofilin isoform to directly demonstrate XAC(wt)-GFP-mediated alterations in actin dynamics in cells (6, 18). With the use of these probes, we manipulated expression of wild-type and mutant XAC-GFP isoforms and studied the effects of their expression on the actin cytoskeleton in proximal tubule cultured cells under physiological and ATP-depleted conditions. Our data indicate a direct role for ADF/cofilin proteins in mediating the severe actin cytoskeletal alterations observed in response to cellular ATP depletion in addition to dramatically impacting the rate and extent of these cellular alterations.

METHODS

Cell culture. Cell culture experiments were performed on three proximal tubule cell lines, two of which were porcine cell lines clonally derived from LLC-PK(wt) (LLC-PK_{10} and LLC-$PK_{A4.8}$), and the S_1 mouse cell line (a kind gift from Dr. G. T. Nagami, Univ. of California at Los Angeles School of Medicine, Los Angeles, CA). The LLC-$PK_{A4.8}$ cell line was maintained in a low-glucose (1 mg/ml glucose) DMEM (Sigma D-5523) containing 10% FBS, 100 U/ml of penicillin, and 100 μg/ml of streptomycin, pH 7.4, at 37°C in 5% CO_2 incubators. The LLC-PK_{10} cell line was maintained and expanded on plastic tissue culture dishes in DMEM (JRH Biosciences, no. 56-498) containing 10% FBS, 100 U/ml of penicillin, and 100 μg/ml of streptomycin, pH 7.4. The S_1 cells were cultured in a 50:50 mixture of Ham's F-12:DMEM supplemented with 2 mM L-glutamine, 10 mM sodium-HEPES, 2 mM sodium pyruvate, insulin, sodium selenite, and sodium bicarbonate and 7% fetal calf serum, penicillin, and streptomycin. For immunofluorescence studies, cells were grown on glass coverslips, whereas cells for protein extraction were grown on plastic dishes. Cells treated for ATP depletion were incubated in 0.1 μM antimycin A diluted in substrate-free DMEM (no glucose, pyruvate, serum, or amino acids), pH 7.4, or in depletion buffer, 1× PBS containing 0.5 mM $CaCl_2$, and 1.0 mM $MgCl_2$, pH 7.4, for designated time intervals.

Adenoviral construction. XAC-GFP (wt, S3A mutant and S3E mutant) clones were constructed in the Clontech phGFP-S65T vector by H. Abe, Chiba University, and generously shared with us. The 1,300-bp XAC-phGFP (wt, S3A and S3E) inserts were removed from the phGFP plasmid with *Sac*I and *Xba*I (*Sac*I site was blunt ended by degrading the 3′

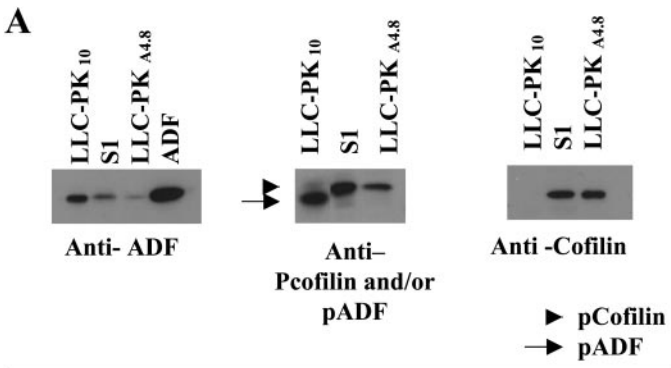

	ADF	pADF	Cofilin	pCofilin
LLC-PK_{10}	+++	+++	-	-
S1	+	+/-	+++	+++
LLC-$PK_{A4.8}$	-	-	+++	+++

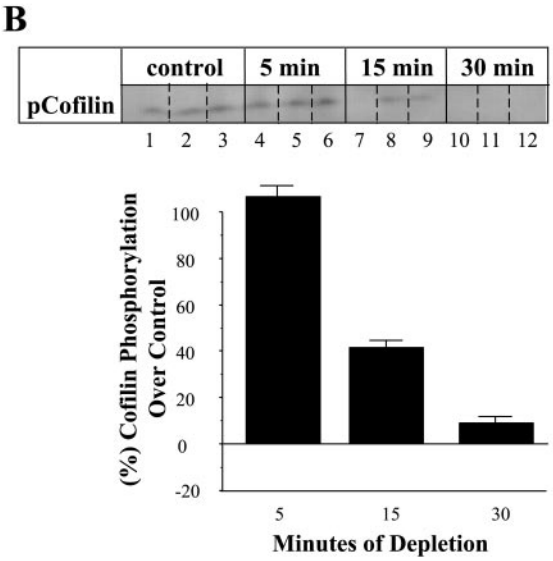

Fig. 1. ATP depletion activates cofilin in LLC-$PK_{A4.8}$ cells. Cellular homogenate proteins (equal amounts) from S_1, LLC-$PK_{A4.8}$, and LLC-PK_{10} cells were probed using isoform-specific antibodies for actin-depolymerizing factor (ADF), cofilin, or the phosphoepitope of phosphorylated (p)ADF and pcofilin, which also recognize pXAC(wt)-green fluorescence protein (GFP). Under physiological conditions, the cofilin isoform was predominately expressed and phosphorylated in LLC-$PK_{A4.8}$ cells, whereas ADF was very low or nonexistent (*A*). In LLC-PK_{10} cells, the expression pattern was reversed, with ADF primarily expressed and phosphorylated, and neither pcofilin nor cofilin was detected. Both isoforms, ADF and cofilin, were expressed and detected in mouse proximal tubule S_1 cells. Western blots of homogenates of LLC-$PK_{A4.8}$ cells ATP depleted for 0, 5, 15, and 30 min in depletion medium containing 0.1 μM antimycin A were probed with an antibody specific for the phosphoepitope of ADF/cofilin (*B*). Equal amounts of total protein (5 μg) were loaded in each lane with 3 replicates for each time point. The concentration of the inactive pcofilin isoform decreased with increasing time of ATP depletion.

overhang with mung bean nuclease). The XAC-phGFP inserts (wt, S3A or S3E) were cloned into the *Xba*I and blunt ended *Kpn*I site of the shuttle vector plasmid for adenovirus production by homologous recombination in HEK-293 cells as previously described (18). The fusion proteins were expressed under control of the immediate early promoter of the cytomegalovirus.

Adenoviral infection. The cells were infected at 40–60% confluency with a viral multiplicity of infection of 25 for 18 h with adenovirus expressing GFP, XAC(wt)-GFP, the constitutively active mutant XAC(S3A)-GFP, or the inactive mutant form XAC(S3E)-GFP. Cell cultures were harvested at 18, 28, and 51 h postinfection with cell extracts prepared and examined by SDS-PAGE, followed by Western blot analysis. By 24 h postinfection, 70–80% of the treated cells were expressing XAC-GFP isoforms as observed by epifluorescence microscopy. All studies were done at 24 h postinfection unless otherwise stated.

SDS-PAGE and Western analysis. LLC-PK or S_1 cellular proteins were extracted in a 2% SDS buffer (2% SDS, 10 mM Tris, pH 7.6, 10 mM NaF, 5 mM DTT, 2 mM EGTA) and boiled. Protein concentration was determined by a filter paper dye-binding assay (19). Equal protein concentrations (5 μg of total extract protein) were loaded in each lane and separated by SDS-PAGE on 15% isocratic gels. For Western blot analysis, separated proteins were transferred to a polyvinylidene fluoride membrane, and the membrane was blocked with 5% nonfat dry milk or 10% newborn calf serum in 1× Tris-buffered saline with Tween. For immunodetection, the rabbit primary antibodies to XAC (1:10,000), to the phosphopeptide epitope of phosphorylated ADF/cofilin [pADF/pcofilin (also recognizes pXAC)] (1:1,000), and to ADF (1:10,000) or mouse primary monoclonal antibody to cofilin (1:5), were utilized and followed by horseradish peroxidase-conjugated goat anti-rabbit or goat anti-mouse secondary antibodies (1:30,000). Protein bands were detected by enhanced chemiluminescence (Pierce, Rockford, IL) or stained with 4-chloro-1-napthol and quantified by densitometry.

Microscopy. LLC-$PK_{A4.8}$ cells were fixed in 4% paraformaldehyde or 3.7% formaldehyde for 1 h and permeabilized with 0.1% Triton X-100. F-actin was stained with rhodamine-phalloidin (Molecular Probes, Eugene, OR; 1:60 dilution) or Texas red-phalloidin (1:200; 1:10). Confocal images were acquired with an MRC-1024 laser-scanning confocal microscope (Bio-Rad, Hercules, CA) using a Nikon Diaphot 200 inverted microscope with a ×100, 1.4-numerical aperture (NA) oil-immersion objective or a ×60, 1.2-NA water-immersion objective. Live cell images were captured with a Nikon Diaphot inverted microscope with a ×40, 0.85-NA objective

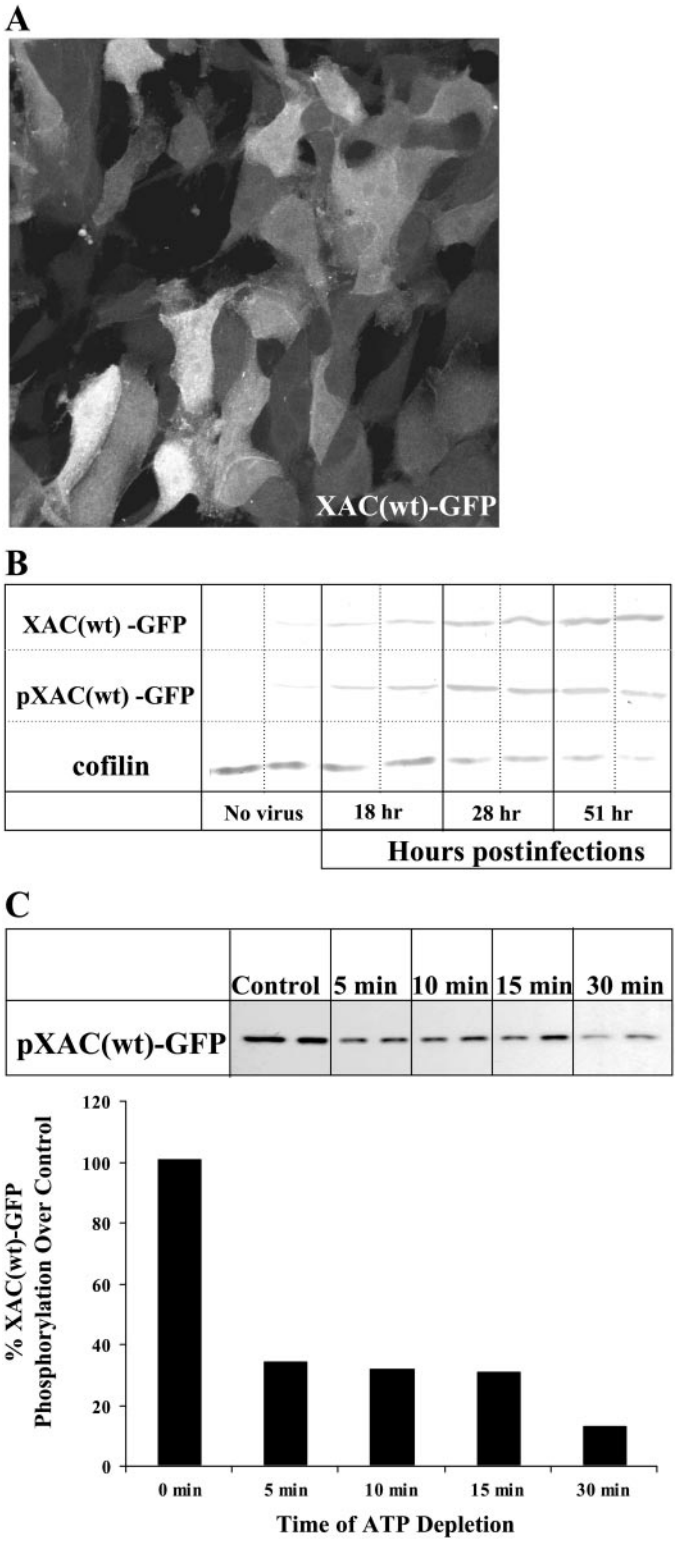

Fig. 2. Adenoviral *Xenopus* ADF/cofilin cDNAs (wild-type) linked to GFP [XAC(wt)-GFP] expression and its phosphorylation increased from 18 to 51 h postinfection with a downregulation of endogenous cofilin. LLC-$PK_{A4.8}$ cell cultures were infected with the adenovirus containing XAC(wt)-GFP with a multiplicity of infection of 25 for 18 h. *A*: 24 h postinfection, 70–90% of the cells showed varying levels of GFP fluorescence as observed by confocal microscopy. Cell cultures were harvested at 18, 28, and 51 h postinfection, and the cell extracts were examined by SDS-PAGE and Western blot analysis loading of 5 μg of total extract protein per lane (*B*). The blots were probed with rabbit anti-XAC, rabbit antibody to the phosphoepitope of ADF, and cofilin, which also recognized pXAC(wt)-GFP or mouse anti-cofilin primary antibodies, followed by horseradish peroxidase-conjugated goat anti-rabbit or goat anti-mouse secondary antibodies. XAC(wt)-GFP expression was observed by Western blot analysis as early as 18 h after adenoviral infection and continued to increase for up to 51 h. An increase in the pXAC(wt)-GFP was also documented during this time frame, suggesting XAC(wt)-GFP could be phosphorylated by a cellular kinase. A decrease in the concentration of endogenous cofilin was noted at 28 h postinfection and remained lower at 51 h postinfection. In response to ATP depletion (Fig. 2*C*), pXAC(wt)-GFP was dephosphorylated, as demonstrated by Western blot analysis of cellular homogenates of XAC(wt)-GFP expressing cultured cells probed with an antibody to pADF/pcofilin that also recognizes the phosphoepitope of 45-kDa pXAC(wt)-GFP.

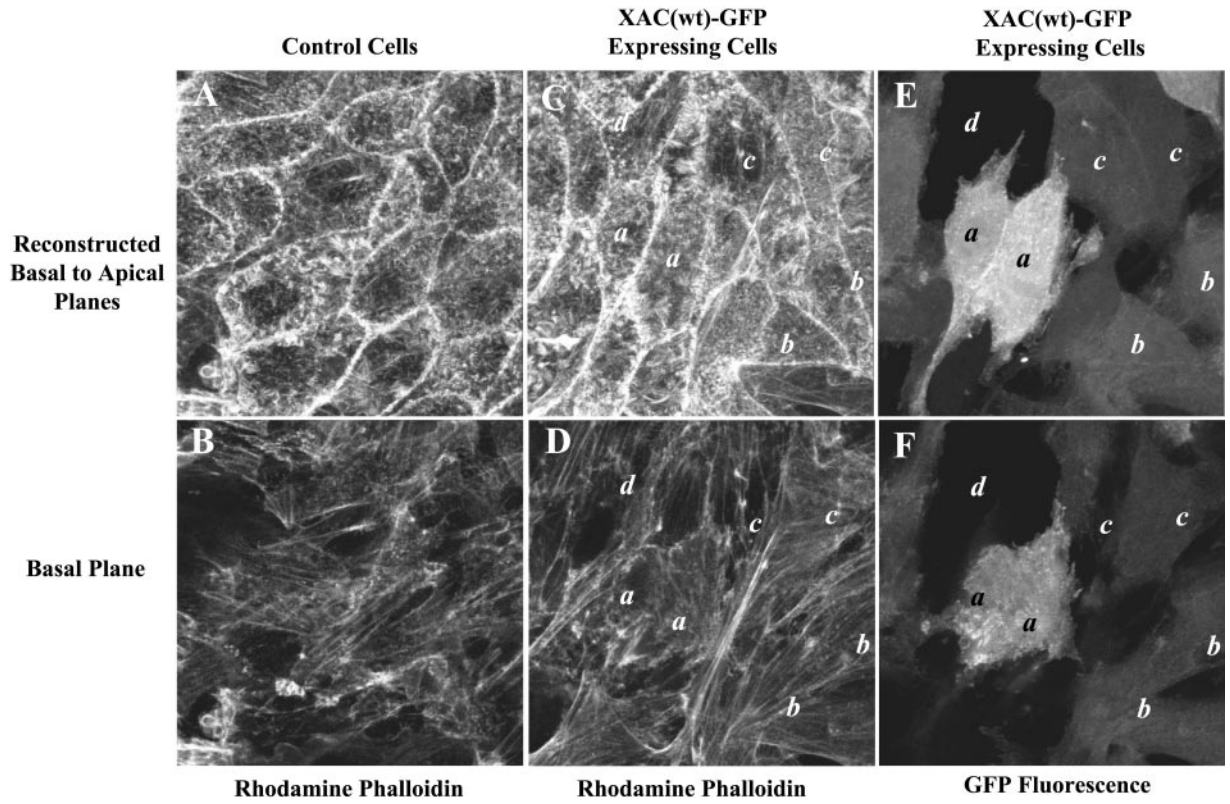

Fig. 3. Actin cytoarchitecture was preserved in adenoviral-infected LLC-PK$_{A4.8}$ cells expressing XAC-GFP under physiological conditions. Rhodamine-phalloidin staining of F-actin in LLC-PK$_{A4.8}$ cells expressing XAC(wt)-GFP (*C* and *D*) did not demonstrate alterations in the F-actin structures compared with uninfected LLC-PK$_{A4.8}$ cells (*A* and *B*) in three-dimensional reconstructed and basal images. The rhodamine-phalloidin-stained, F-actin-bundled stress fibers in the control cells (*B*) were similar in size and frequency to those of the XAC(wt)-GFP-expressing LLC-PK$_{A4.8}$ cells (*D*). In the reconstructed images, microvillar actin present in noninfected cells (*A*) was comparable in number, size, and intensity as in XAC(wt)-GFP-infected cells (*C*). To demonstrate different levels of XAC(wt)-GFP expression and its effect on actin organization, GFP fluorescent cells shown in images *E* and *F* (high expression, *a*; medium expression, *b*; low expression, *c*; and no expression, *d*) can be compared with their corresponding rhodamine-phalloidin-stained F-actin images in *C* and *D*. No notable difference in the actin stress fibers or apical microvillar actin could be discerned between higher XAC(wt)-GFP-expressing cells (*a*) compared with lower expressing cells (*b* and *c*) or nonexpressing cells (*d*).

and a PXL cooled charge-coupled device camera with a Kodak 1400 chip (Photometrics, Tucson, AZ). Metamorph software (Universal Imaging, West Chester, PA) was used to process the images and to reconstruct basal-to-apical three-dimensional reconstructions.

RESULTS

ATP depletion of LLC-PK$_{A4.8}$ cells reduces pcofilin signal. Initial studies were undertaken to determine the effect of ATP depletion on the phosphorylation status of cofilin in LLC-PK$_{A4.8}$ cells. ADF and cofilin are two highly conserved and related proteins, but differentially expressed proteins with similar, but distinct, actin-binding properties belonging to the same family of actin-associated proteins (5, 32). With the use of isoform-specific antibodies and an anti-phosphoepitope antibody that recognizes the phosphorylated form of each isoform, the cellular expression of these proteins can be determined. With the use of these probes, we found that the endogenous expression of ADF and cofilin isoforms in porcine proximal tubule cell lines was not equivalent. The LLC-PK$_{4.8}$ cells had ample expression of cofilin and little or no expression of ADF (Fig. 1*A*). The LLC-PK$_{10}$ cell line expressed ADF with no expression of cofilin, whereas the S$_1$ mouse cell line expressed both isoforms.

As shown in Fig. 1*B*, antimycin A-induced ATP depletion of LLC-PK$_{4.8}$ cells diminished the pcofilin signal in a time-dependent manner consistent with previously published in vivo rat kidney data that demonstrated ischemia induced a time-dependent dephosphorylation of phosphorylated ADF (29). Induction of ATP depletion for 5 min had no effect on cofilin phosphorylation, but within 15 min, a 60% decrease was observed in pcofilin concentration. By 30 min of ATP depletion, pcofilin had been reduced to <10%. As there was no change in total cellular cofilin (data not shown), these data imply that ATP depletion induced a rapid duration-dependent dephosphorylation of cofilin.

Expression of XAC-GFP through adenoviral infection of LLC-PK$_{A4.8}$ cells. To obtain direct evidence regarding the role of cofilin-mediated cellular actin destruction and reorganization and microvillar F-actin core

degeneration during ATP depletion, we utilized adenoviral vectors containing GFP, XAC(wt)-GFP, XAC(S3A)-GFP, or XAC(S3E)-GFP cDNA to express GFP or ADF/cofilin protein isoforms in LLC-PK$_{A4.8}$ cells. In characterization studies, LLC-PK$_{A4.8}$ cells infected with adenovirus containing the cDNA for XAC(wt)-GFP demonstrated expression of the XAC(wt)-GFP fusion protein as early as 18 h postinfection, as detected by GFP fluorescence (Fig. 2*A*) and Western blotting techniques (Fig. 2*B*). The fraction of GFP-expressing cells increased from ~70 to 90% over the 51-h period postinfection (Fig. 2*A*). The level of XAC(wt)-GFP expression increased linearly over the 51-h period postinfection (Fig. 2*B*). The level of phosphorylated XAC(wt)-GFP, as detected by Western blot analysis, also increased linearly over the 51-h period postinfection (Fig. 2*B*). Therefore, as the wild-type XAC-GFP protein was expressed, it was regulated through phosphorylation by a cellular kinase. The level of endogenous cofilin, as detected by Western blot analysis, remained constant during the first 18 h postinfection of XAC(wt)-GFP, but decreased endogenous cofilin levels were observed at 28 and 51 h postinfection.

ATP depletion resulted in rapid dephosphorylation of pXAC(wt)-GFP (Fig. 2*C*), as was seen for endogenous pcofilin (Fig. 1*B*). Compared with control levels, there was a 60% decrease in pXAC(wt)-GFP in response to 5 min of ATP depletion, which was further reduced to 10% pXAC(wt)-GFP at 30 min of ATP depletion, showing dephosphorylation by an endogenous phosphatase. Together, these data indicate that ample expression, physiological phosphorylation, and dephosphorylation, in response to ATP depletion of XAC(wt)-GFP, occurred at the cellular level. Endogenous cofilin was also downregulated in response to XAC(wt)-GFP expression.

XAC-GFP expression did not alter F-actin under physiological conditions. To determine the effect of XAC(wt)-GFP expression on the F-actin cytoskeleton of LLC-PK$_{A4.8}$ cells, cells were stained with rhodamine or Texas red-phalloidin 24 h postinfection with adenovirus containing XAC(wt)-GFP. In Fig. 3, *A*–*F*, reconstructed basal-to-apical images and single-plane basal images of uninfected control cells (*A* and *B*) and XAC(wt)-GFP-expressing cells (*C*–*F*) are presented. In Fig. 3, *C*–*F*, comparison of actin cytoskeletal stress fibers, microvillar microfilaments, and cortical actin network can be drawn between high (*a*), medium (*b*), and low (*c*) XAC(wt)-GFP-expressing cells and nonexpressing cells (*d*). These data demonstrate that adenoviral infection and XAC(wt)-GFP expression did not affect the distribution or composition of the dense F-actin bundles that compose basal stress fibers, apical microvillar microfilament cores, or the cortical actin orientation of LLC-PK$_{A4.8}$ cells, suggesting XAC(wt)-GFP expression does not alter cellular actin architecture under physiological conditions, implying physiological regulation and function of the XAC(wt)-GFP proteins.

XAC(wt)-GFP translocates to the surface membrane domain in response to ATP depletion. Basal-to-apical reconstructions (*x-z* axes images) demonstrate that, under physiological conditions (Fig. 4*A*), F-actin primarily located to basal and lateral aspects of the cell and in the microvilli at the apical surface. The expression of XAC(wt)-GFP under physiological conditions (Fig. 4*B*) was primarily detected in the cytoplasm of the LLC-PK$_{A4.8}$ cells with little or no colocalization of fluorescence with Texas red-phalloidin F-actin staining in the apical, basal, or lateral cellular regions. However, XAC(wt)-GFP-expressing cells that were ATP depleted for 25 min (Fig. 4*C*) had intense XAC(wt)-GFP fluorescence, and colocalization of XAC(wt)-GFP with F-actin staining in the apical and basal aspects of the cell. Also, F-actin and XAC(wt)-GFP were colocalized to dense aggregates (multiple orange/yellow areas) in the cytoplasm. These data are in agreement with and extend our previous observations showing rapid relocal-

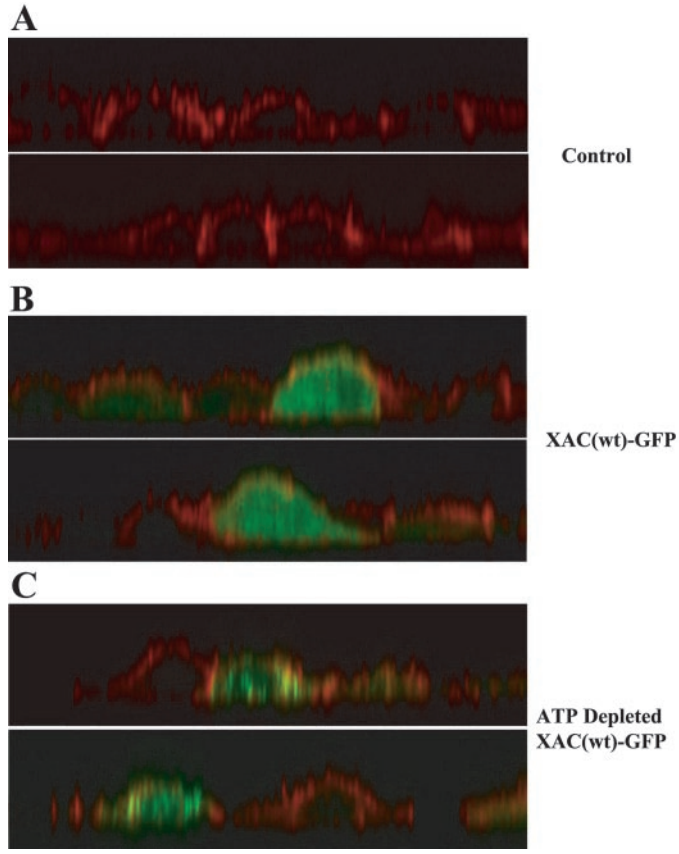

Fig. 4. ATP depletion induced surface membrane localization of XAC-GFP. Untreated uninfected XAC(wt)-GFP-expressing and ATP-depleted XAC(wt)-GFP-expressing LLC-PK$_{A4.8}$ were stained with Texas red-phalloidin, and through-focus images were taken. Metamorph software was used to reconstruct basal-to-apical images. These three-dimensional (*x-z* or *y-z* axes) reconstructed vertical slice images of control and ATP-depleted LLC-PK$_{A4.8}$ cells demonstrated that under physiological conditions, F-actin localized to the cortical aspects of the cell and in the microvilli at the apical surface (*A*). Under physiological conditions, the fluorescent signal for XAC(wt)-GFP was primarily detected in the cytoplasm of cultured cells with little or no fluorescence in the apical aspects of the cell (*B*). XAC(wt)-GFP-expressing cells that were ATP depleted for 25 min demonstrated a significant increase in the cytoplasmic XAC(wt)-GFP fluorescence colocalizing (yellow) with F-actin in the surface membrane regions and in aggregates in the cytosol (*C*).

ization of ADF to the apical domain of rat proximal tubule cells during ischemia (3).

XAC mediates F-actin aggregation and rod formation during ATP depletion. We next sought to determine the effect of XAC expression and ATP depletion on the F-actin cytoskeleton. Cell monolayers infected with the XAC(wt)-GFP adenovirus were ATP depleted with antimycin A in depletion media for 25 min and stained for F-actin using Texas red-phalloidin (1:10). In Fig. 5, *A–C*, both XAC(wt)-GFP-expressing and uninfected cells (arrows) were present in the same monolayer. Uninfected cells, ATP depleted for 25 min (Fig. 5, *A–C*, arrows), were characterized by minimal disturbance in the fine-mesh cortical and stress fiber F-actin staining (Fig. 5*A*, arrow). These data are similar to what we previously described under physiological or short-term, ATP-depleted conditions (24). However, in XAC(wt)-GFP-expressing neighboring cells undergoing ATP depletion, intracellular F-actin disruption and aggregation were readily seen, with higher XAC(wt)-GFP-expressing cells being disrupted to a greater extent than cells with lower expression levels. Colocalization of XAC(wt)-GFP and F-actin, as demonstrated by intense yellow fluorescence (Fig. 5*C*, open square), was apparent in XAC(wt)-GFP-expressing cells. The F-actin- and XAC-GFP-stained aggregates had a much brighter GFP signal than the Texas red-phalloidin F-actin signal. We believe this difference in staining properties results from the known competition between XAC-GFP and phalloidin for F-actin binding (5, 17).

To evaluate whether rod and aggregate formation, in response to ATP depletion in XAC(wt)-GFP-expressing cells, was a direct result of XAC(wt)-GFP-mediated actin alterations, we expressed either the constitutively active mutant XAC(S3A)-GFP, the inactive mutant XAC(S3E)-GFP, or GFP in LLC-$PK_{A4.8}$ cells. No rods or aggregates formed in the GFP (Fig. 6, *A–C*) or S3E mutant-infected cells (Fig. 6, *D–F*), even when ATP depleted for 30 min. These data support the hypothesis that the active ADF/cofilin isoform directly mediates breakdown of the actin cytoskeleton, leading to formation of ADF/cofilin aggregates and rods, whereas the inactive isoform cannot induce these events. These data further support a role for the dephosphorylated and activated ADF/cofilin proteins mediating the cellular actin changes observed with ATP depletion during renal ischemia. Expression of the constitutively active isoform led to spontaneous disruption of the actin cytoskeleton, with formation of rods and aggregates often resulting in detachment or cell death by 24 h postinfection (Fig. 6, *G–I*). In addition, we observed a reduction in cellular stress fibers in cells expressing the constitutively active mutant.

ATP depletion induces rapid formation of aggregates and rods in cells expressing XAC(wt)-GFP. Next, we sought to determine the time course of F-actin alterations in control and XAC(wt)-GFP-expressing cells in response to ATP depletion. Rapid and extensive appearance of XAC-GFP/F-actin aggregates and rods would directly indicate an important and early role for ADF/cofilin proteins in mediating F-actin disruption. To test this hypothesis, we undertook ATP depletion studies of cells infected with either XAC(wt)-GFP, GFP, or XAC(S3E)-GFP. In GFP- and XAC(S3E)-GFP-expressing cells, as well as in uninfected cells, we did not observe alterations to the actin cytoskeleton comparable with the severe alterations observed in XAC(wt)-GFP-expressing cells in response to the same time of ATP depletion (Figs. 5 and 6). XAC(wt)-GFP-, GFP-, and XAC(S3E)-GFP-expressing cells all demonstrated a high percentage of GFP signal, indicating a

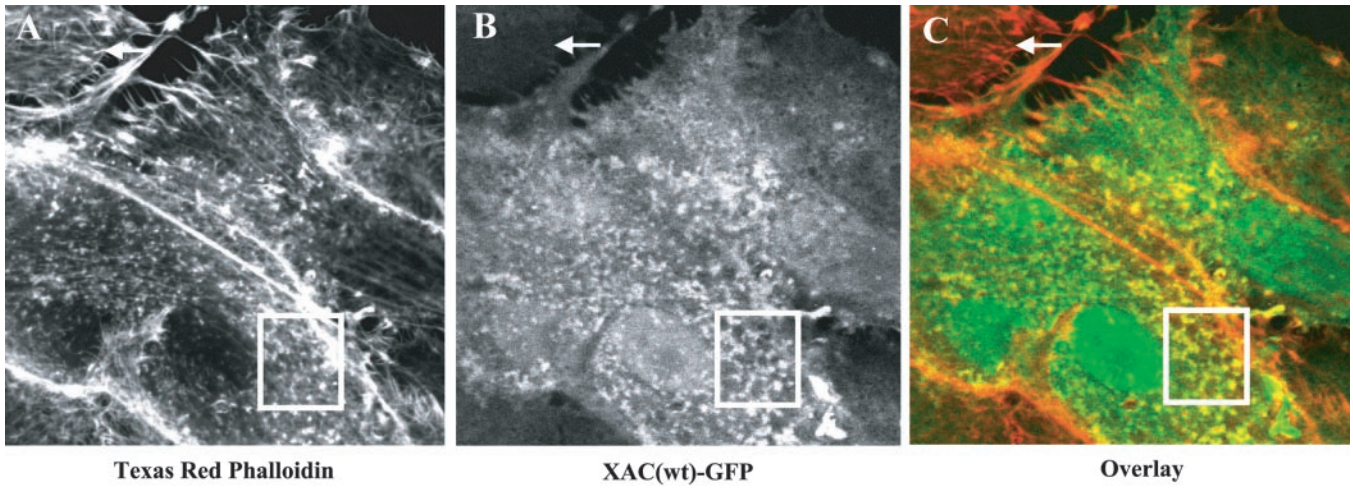

Fig. 5. ATP depletion induces formation of actin aggregates and rods in XAC(wt)-GFP-expressing cells. Twenty-five minutes of ATP depletion of LLC-$PK_{A4.8}$ cells expressing XAC(wt)-GFP with 0.1 μM antimycin A in depletion buffer induced rapid and extensive formation of aggregates (small square in *A–C*) characterized by Texas red-phalloidin staining (*A*) and XAC(wt)-GFP fluorescence (*B*). Uninfected cells in the same monolayer (arrow in *A–C*) did not demonstrate any comparable changes to their cytoskeletal structure, although they underwent the same ischemic insult. Merged images (*C*) demonstrate that the aggregates contain both XAC(wt)-GFP and F-actin through the colocalization of XAC(wt)-GFP signal with Texas red-phalloidin signal.

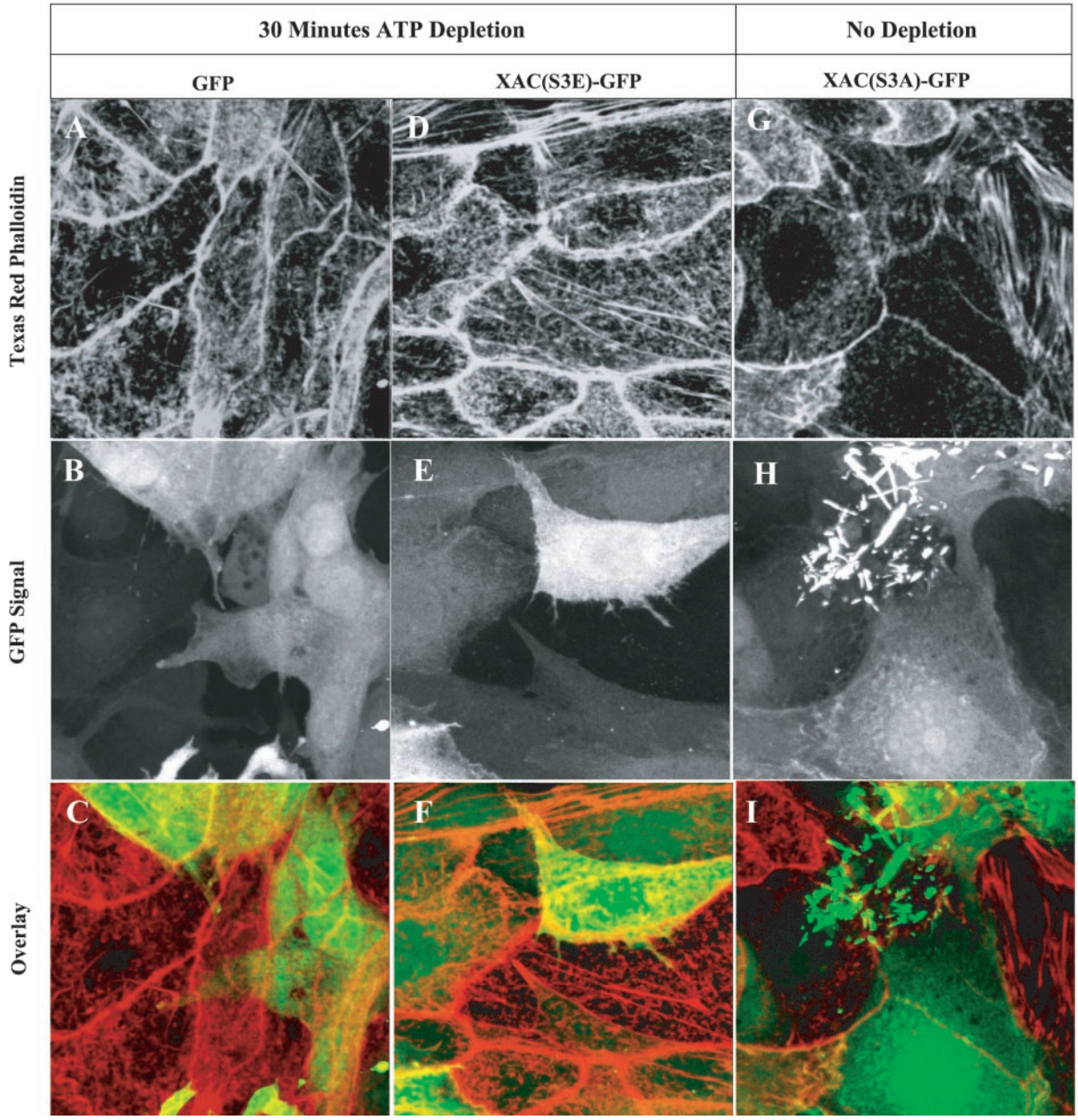

Fig. 6. Aggregates and rods do not form in response to ATP depletion of LLC-PK$_{A4.8}$ cells expressing GFP or XAC(S3E)-GFP but spontaneously form in nondepleted XAC(S3A)-GFP-expressing cells. LLC-PK$_{A4.8}$ cultured cells infected with adenovirus containing the cDNA for GFP (*A–C*) and for the constitutively inactive mutant XAC(S3E)-GFP (*D–F*) were ATP depleted for 30 min and stained with Texas red-phalloidin to analyze their actin cytoskeleton. Close examination of the actin stress fibers and microvilli did not demonstrate any notable differences between GFP- or XAC(S3E)-GFP-expressing cells and noninfected cells. However, LLC-PK$_{A4.8}$ cultured cells infected with adenovirus containing the cDNA for the constitutively active XAC(S3A)-GFP isoform (*G–I*) demonstrated spontaneous cytoskeletal changes. The actin stress fibers and microvilli were disrupted with formation of aggregates and rods, with many infected cells breaking apart and lifting from the coverslip.

similar level of infection and GFP protein expression. In addition, the wild-type XAC(wt)-GFP-expressing cells appeared similar in morphology to uninfected cells or cells infected with GFP or the inactive S3E mutant. During ATP depletion, the GFP intensity and distribution at 2 min were comparable in the XAC(wt)-GFP-, GFP-, XAC(S3E)-GFP-expressing cells (Fig. 7, *A*, *D*, and *G*). A homogenous cytosolic distribution of GFP was observed, and nuclear localization was also noted. By 10 min of ATP depletion, localization of the GFP signal began to change in the XAC(wt)-GFP-expressing cells but not in the GFP- or XAC(S3E)-GFP-expressing cells (data not shown). By 20 min, cells expressing XAC(wt)-GFP had a reduction in the homogenous cytosolic XAC(wt)-GFP signal and an accumulation of cytoplasmic XAC(wt)-GFP-stained aggregates (Fig. 7*B*,

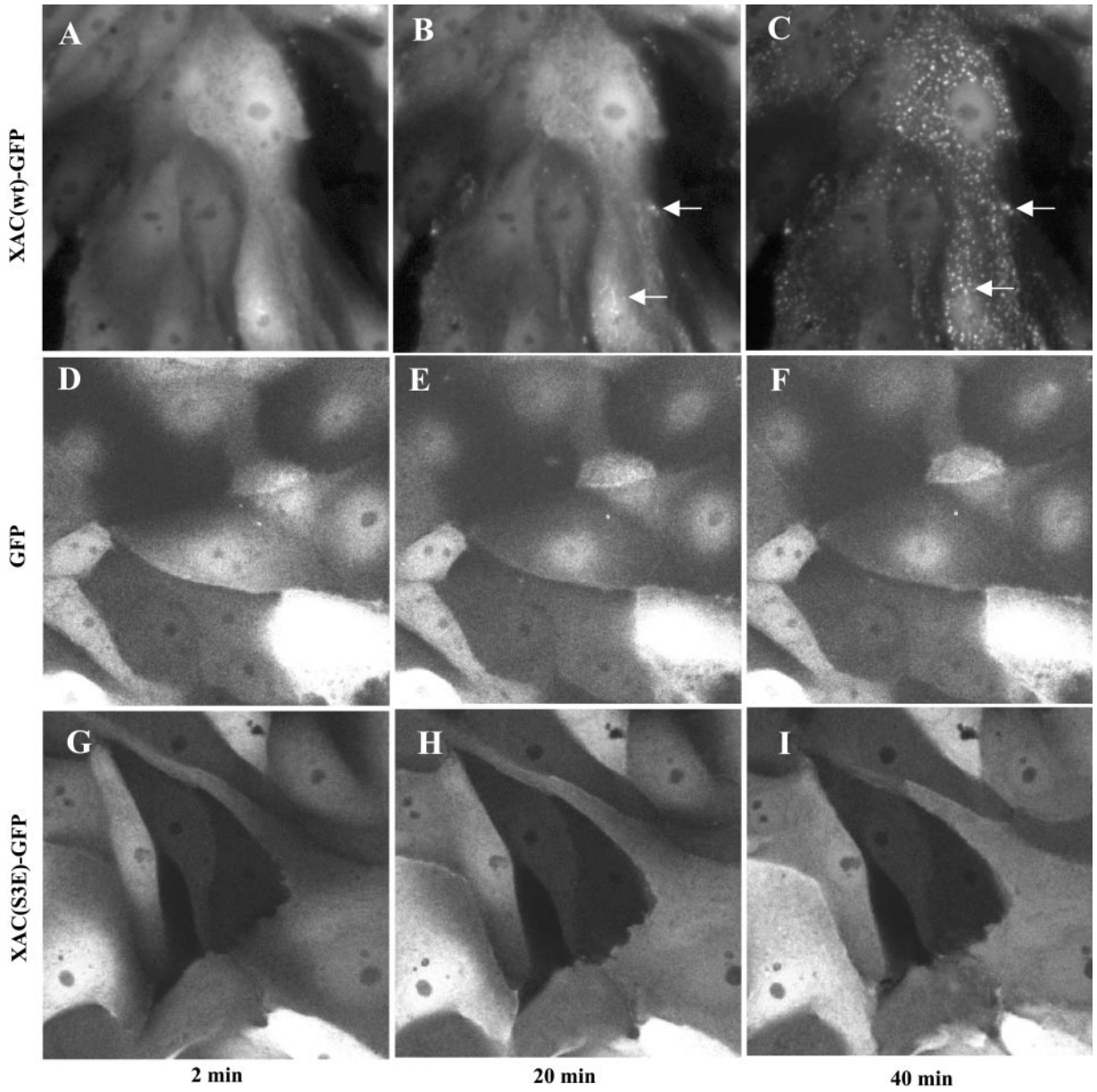

Fig. 7. ATP depletion of LLC-PK$_{A4.8}$ cells expressing XAC(wt)-GFP rapidly induced formation of rods and aggregates of XAC(wt)-GFP. LLC-PK$_{A4.8}$ cells infected with adenovirus containing either XAC(wt)-GFP, GFP, or XAC(S3E)-GFP were ATP depleted in depletion buffer containing 0.1 μM antimycin A and observed for 40 min. During the first 10 min of ATP depletion, GFP-stained aggregates formed in the XAC(wt)-GFP- (*A–C*) but not the GFP (*D–F*)- or XAC(S3E)-GFP (*G–I*)-expressing cells. By 20 min of ATP depletion, the XAC(wt)-GFP signal was observed in large clumps (arrows) in most cells (*B*) expressing XAC(wt)-GFP, but not in the GFP (*E*) or S3E mutant- (*H*) expressing cells (*E*). As XAC(wt)-GFP-stained rod and aggregate (arrows) formation continued in the XAC(wt)-GFP-expressing cells, the diffuse cytoplasmic XAC(wt)-GFP staining decreased (*B*). By 40 min, this effect was further enhanced in the XAC(wt)-GFP-expressing cells (*C*). In contrast, depletion of the cells infected with GFP (*D–F*) or the XAC(S3E)-GFP constitutively inactive mutant-expressing cells did not demonstrate any notable changes in the diffuse GFP staining observed under control conditions.

arrows). By 40 min, this effect was further enhanced in the XAC(wt)-GFP-infected cells (Fig. 7*C*), but the GFP- and XAC(S3E)-GFP-expressing cells still demonstrated no change in the diffuse GFP fluorescence (Fig. 7, *F* and *I*).

DISCUSSION

This is the first study to directly demonstrate that the ADF/cofilin family of proteins mediates dramatic alterations to actin filament cytoarchitecture in response to ATP depletion. The ADF/cofilin family of proteins orchestrates actin dynamics primarily through accelerating the rate of pointed-end F-actin depolymerization and by severing long F-actin filaments (5). To mediate cellular changes in actin dynamics, these stimulus/responsive proteins preferentially bind ADP-charged F-actin in a pH-dependent manner (7, 8, 11, 16). The ADF/cofilin proteins substantially

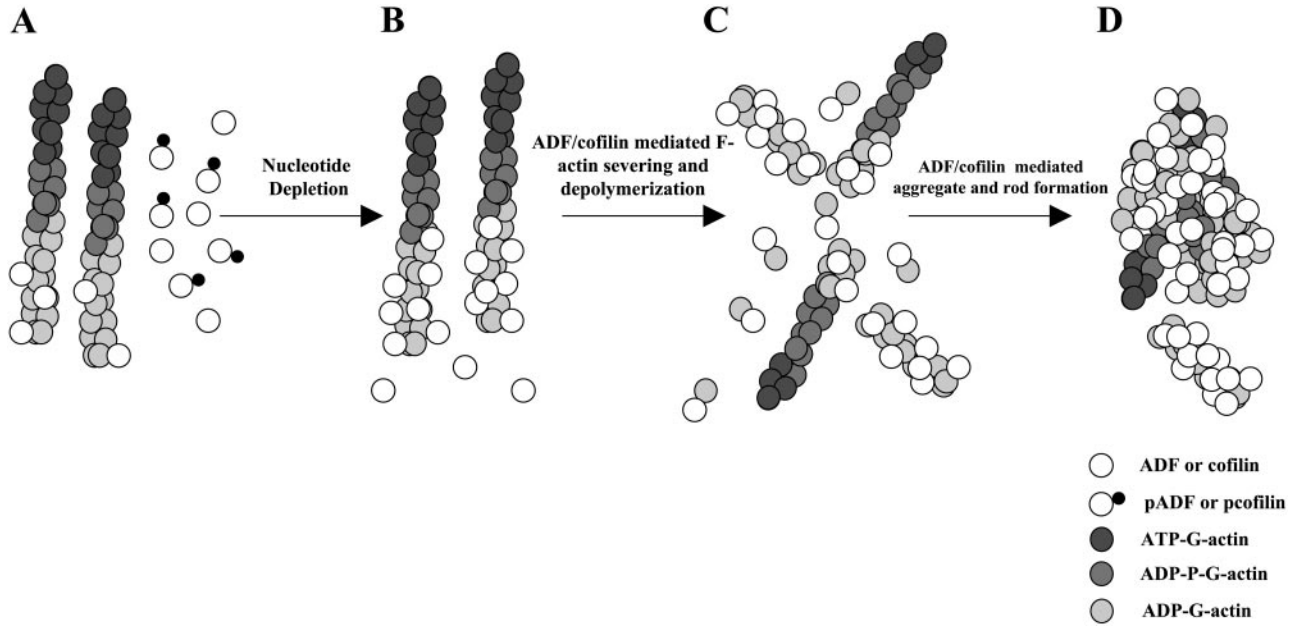

Fig. 8. Model for actin aggregate formation during ATP depletion. Under physiological conditions, F-actin and the proteins of the ADF/cofilin family, in conjunction with other actin-binding proteins, interact in a regulated manner to maintain the F-actin architecture of the cell. Through actin subunit treadmilling and ATP hydrolysis, the actin filaments are polarized with ATP-actin subunits at the barbed end and ADP-actin subunits at the pointed end. Activity of the ADF/cofilin protein family is regulated by phosphorylation. Under physiological conditions, both the active and inactive phosphorylated forms are present (*A*). Ischemia in vivo or ATP depletion in vitro induces pADF/pcofilin dephosphorylation/activation, leading to ADF/cofilin proteins cooperatively binding to the ADP-actin subunits of F-actin (*B*). Once bound to F-actin, ADF/cofilin proteins sever long actin filaments and accelerate F-actin pointed-end depolymerization, producing both ADF/cofilin:ADP-actin dimers and ADF/cofilin proteins bound to F-actin fragments (*C*). We postulate that the lack of cellular ATP results in unregulated ADF/cofilin-mediated F-actin destruction followed by ADF/cofilin-actin aggregate formation (*D*).

increase the polymerization rate of actin, with ADP-actin polymerization affected to a greater extent than ATP-actin polymerization (11). The actin-binding properties of this family of proteins are primarily regulated by phosphorylation and dephosphorylation. Also, ADF/cofilin proteins compete for F-actin binding with other actin-binding proteins and phalloidin. Two kinase families have been identified to specifically phosphorylate ADF/cofilin on serine-3, each with different upstream regulators. The Lim kinase family, the first identified ADF/cofilin-specific kinase, is phosphorylated, and its kinase activity is significantly increased through downstream effects of the Rho family of small GTPases, Rac, Rho, and Cdc42. In turn, the activated Lim kinase phosphorylates and inactivates the ADF/cofilin protein family (2, 34). The second family of ADF/cofilin-specific kinases, the testicular protein kinase family (TESK1 or TESK2), includes serine/threonine kinases stimulated through the integrin-mediated signaling pathway (31). Phosphorylated ADF/cofilin proteins can no longer bind F- or G-actin to regulate actin dynamics (9, 25). Recently, the ADF/cofilin-specific phosphatase slingshot has been shown to dephosphorylate and activate ADF/cofilin at serine-3 (26).

Our previous studies suggested the ADF/cofilin family of proteins played a significant role in ischemia-induced renal cell injury of proximal tubule cells (3, 29). Acute renal failure mediates functional changes in the biochemical, physiological, and morphological aspects of proximal tubule cells (30). The extent of these cellular alterations depends on the time and severity of the cellular injury, with apical membrane microvilli being extremely sensitive because they contain the majority of F-actin in these cells (14, 15, 24). Clinical consequences resulting from ischemic injury include tubular obstruction from apical membrane blebbing, back-leak between cells that have loss their junctional complex integrity, reduced Na^+ reabsorption from redistribution of ion pumps in the membrane, and abnormal tubuloglomerular feedback (30).

Changes in the actin cytoarchitecture occur early and precede the other observed biochemical, functional, and structural alterations, suggesting actin changes are, in part, responsible for the subsequent destructive cellular changes. Within 5 min of renal artery clamping, we observed dephosphorylation/activation of ADF, along with localization of this small protein into the apical microvillar region of the proximal tubule cell, where F-actin staining patterns show initial alterations (3). By 15 min of ischemia-induced injury, the apical membrane begins to coalesce and form luminal or cytoplasmic blebs or vesicles containing high concentrations of ADF and G-actin. In addition, microvillar microfilament destruction is concurrent with increased G-actin concentration in the apical membrane region. These events occur in a time frame

to suggest that ADF locates to this region to participate through F-actin severing and depolymerization in the breakdown of the microvillar microfilament core. In addition to microvillar microfilament changes, aggregates of F-actin have been observed in the cytoplasm of injured proximal tubule cells (12, 15, 24).

Although our previous studies suggested dephosphorylation/activation and relocalization of ADF were coincident with microvillar microfilament core disintegration in response to ischemic injury, we could not directly test the involvement of ADF in this process. Therefore, to directly evaluate the role of the ADF/cofilin family of proteins in proximal tubule cell actin alterations, we expressed the ADF/cofilin isoform XAC(wt)-GFP by adenoviral infection in the proximal tubule cultured cell line LLC-$PK_{A4.8}$. In these cells, endogenous cofilin expression is $<0.1\%$ of the total protein concentration (data not shown). With expression of XAC(wt)-GFP, we observed a decrease in endogenous cofilin levels, suggesting that endogenous cofilin played a minimal role in actin alterations in response to ATP depletion in XAC(wt)-GFP LLC-$PK_{A4.8}$-expressing cells. Although expression of GFP, XAC(S3E)-GFP, or XAC(wt)-GFP in these cells did not alter the integrity of their actin cytoskeleton, inducing ATP depletion in the XAC(wt)-GFP-expressing cells resulted in extremely rapid and extensive changes in the actin cytoarchitecture (Figs. 3, 5, and 6) comparable to the phenotype observed in uninfected cells that underwent a much longer ischemic insult (12). XAC(wt)-GFP-containing aggregates and rods appeared within 10 min of ATP depletion and increased in number and size with depletion time. Actin aggregates were not observed in uninfected cells until after >30 min of ATP depletion. These aggregates were primarily located in the cytoplasm, although rods were also observed in the nucleus. As the number of XAC(wt)-GFP/actin aggregates increased, stress fibers and the fine meshwork of the cortical F-actin disappeared, suggesting XAC(wt)-GFP bound F-actin to depolymerize, sever, and redistribute the characteristic F-actin meshwork into dense aggregates of F-actin bound by XAC(wt)-GFP. Because XAC(wt)-GFP competes with phalloidin for F-actin binding, increased concentrations of Texas red-phalloidin were utilized to insure phalloidin binding and, therefore, visualization of F-actin. Also, with ATP depletion, the XAC(wt)-GFP relocalized into basal and apical regions of the cells. Therefore, with ATP depletion, XAC(wt)-GFP signal significantly increased and rapidly moved from a diffuse cytoplasmic distribution into aggregates along with F-actin. To achieve this remodeling, XAC(wt)-GFP must be activated from its predepletion state and relocalized to bind F-actin with subsequent F-actin depolymerization and severing activity, followed by localization of XAC(wt)-GFP along with F-actin to new abnormal actin aggregate and rod structures (Fig. 8). These data extend our kidney in vivo studies by providing direct evidence that XAC(wt)-GFP relocalizes and participates in F-actin destruction and remodeling. Finally, in cells infected with the constitutively active form of XAC(S3A)-GFP, spontaneously occurring aggregates and rods were seen postinfection, and 24 h later, the entire actin cytoskeleton was disrupted. This resulted in cell detachment and death (Fig. 6). These data, and the lack of F-actin disruption in response to ATP depletion in GFP- and XAC(S3E)-GFP-expressing cells (Fig. 6), further demonstrate that activation of ADF/cofilin is required to bring about these cytoskeletal alterations.

The mechanism for formation of ADF/cofilin rods and aggregates is unknown, although recent studies by Pfannstiel and coworkers (27) suggest cofilin oligomers may induce actin bundling activity, leading to aggregate formation. At present, there are no data to support this in LLC-$PK_{A4.8}$ cells that have been ATP depleted. Although it is possible that XAC(wt)-GFP proteins may form oligomers in response to long-term ATP depletion in oxidizing conditions, short-term ATP depletion results in a drop in intracellular pH that is not consistent with reported conditions for cofilin oligomer formation (27).

In summary, these studies strongly suggest ATP depletion induced ADF dephosphorylation/activation and relocalization to mediate F-actin alterations. By expressing the ADF/cofilin protein, and through its GFP fluorescent tag, we were able to follow its activity in response to ATP depletion. With the use of this powerful tool, we demonstrated that ATP depletion rapidly stimulated movement of the XAC(wt)-GFP signal from a diffuse cytoplasmic distribution to localize at sites of F-actin and to newly formed actin aggregates and rod structures. These data strongly suggest XAC(wt)-GFP bound, depolymerized, and severed F-actin to remodel actin into XAC(wt)-GFP-containing aggregates and rods. These data further substantiate a mechanistic role for ADF/cofilin proteins in mediating the rapid actin cytoskeletal remodeling that leads to the functional changes observed in the biochemical, physiological, and morphological aspects of the proximal tubule cells in response to ischemia-induced injury.

We thank Laurie Minamide and Melanie Hosford for technical expertise and helpful discussions.

This research was supported by National Institutes of Health (NIH) Grants 1P01-DK-53465, 1R01-DK-41126, and Veterans Affairs Merit Review grants (to B. A. Molitoris), American Paralysis Association Grant BB2-9601 (to P. J. Meberg), and NIH Grants GM-35126 and NS-40371 (to J. R. Bamburg).

REFERENCES

1. **Abe H, Obinata T, Minamide LS, and Bamburg JR.** *Xenopus laevis* actin-depolymerizing factor/cofilin: a phosphorylation-regulated protein essential for development. *J Cell Biol* 132: 871–885, 1996.
2. **Arber S, Barbayannis FA, Hanser H, Schneider C, Stanyon CA, Bernard O, and Caroni P.** Regulation of actin dynamics through phosphorylation of cofilin by LIM-kinase. *Nature* 393: 805–809, 1998.
3. **Ashworth SL, Sandoval RM, Hosford M, Bamburg JR, and Molitoris BA.** Ischemic injury induces ADF relocalization to the apical domain of rat proximal tubule cells. *Am J Physiol Renal Physiol* 280: F886–F894, 2001.
4. **Bacallao R, Garfinkel A, Monke S, Zampighi G, and Mandel LJ.** ATP depletion: a novel method to study junctional

properties in epithelial tissues. I. Rearrangement of the actin cytoskeleton. *J Cell Sci* 107: 3301–3313, 1994.
5. **Bamburg JR.** Proteins of the ADF/cofilin family: essential regulators of actin dynamics. *Annu Rev Cell Dev Biol* 15: 185–230, 1999.
6. **Bernstein BW, Painter WB, Chen H, Minamide LS, Abe H, and Bamburg JR.** Intracellular pH modulation of ADF/cofilin proteins. *Cell Motil Cytoskeleton* 47: 319–336, 2000.
7. **Blanchoin L and Pollard TD.** Interaction of actin monomers with *Acanthamoeba* actophorin (ADF/cofilin) and profilin. *J Biol Chem* 273: 25106–25111, 1998.
8. **Blanchoin L and Pollard TD.** Mechanism of interaction of *Acanthamoeba* actophorin (ADF/cofilin) with actin filaments. *J Biol Chem* 274: 15538–15546, 1999.
9. **Blanchoin L, Robinson RC, Choe S, and Pollard TD.** Phosphorylation of *Acanthamoeba* actophorin (ADF/cofilin) blocks interaction with actin without a change in atomic structure. *J Mol Biol* 295: 203–211, 2000.
10. **Canfield PE, Geerdes AM, and Molitoris BA.** Effect of reversible ATP depletion on tight-junction integrity in LLC-PK_1 cells. *Am J Physiol Renal Fluid Electrolyte Physiol* 261: F1038–F1045, 1991.
11. **Carlier MF, Laurent V, Santolini J, Melki R, Didry D, Xia GX, Hong Y, Chua NH, and Pantaloni D.** Actin depolymerizing factor (ADF/cofilin) enhances the rate of filament turnover: implication in actin-based motility. *J Cell Biol* 136: 1307–1323, 1997.
12. **Fish EM and Molitoris BA.** Extracellular acidosis minimizes actin cytoskeletal alterations during ATP depletion. *Am J Physiol Renal Fluid Electrolyte Physiol* 267: F566–F572, 1994.
13. **Kellerman PS and Bogusky RT.** Microfilament disruption occurs very early in ischemic proximal tubule cell injury. *Kidney Int* 42: 896–902, 1992.
14. **Kellerman PS, Clark RAF, Hoilien CA, Linas SL, and Molitoris BA.** Role of microfilaments in maintenance of proximal tubule structural and functional integrity. *Am J Physiol Renal Fluid Electrolyte Physiol* 259: F279–F285, 1990.
15. **Kroshian VM, Sheridan AM, and Lieberthal W.** Functional and cytoskeletal changes induced by sublethal injury in proximal tubular epithelial cells. *Am J Physiol Renal Fluid Electrolyte Physiol* 266: F21–F30, 1994.
16. **Maciver SK and Weeds AG.** Actophorin preferentially binds monomeric ADP-actin over ATP-bound actin: consequences for cell locomotion. *FEBS Lett* 347: 251–256, 1994.
17. **McGough A, Pope B, Chiu W, and Weeds A.** Cofilin changes the twist of F-actin: implications for actin filament dynamics and cellular function. *J Cell Biol* 138: 771–781, 1997.
18. **Meberg PJ and Bamburg JR.** Increase in neurite outgrowth mediated by overexpression of actin depolymerizing factor. *J Neurosci* 20: 2459–2469, 2000.
19. **Minamide LS and Bamburg JR.** A filter paper dye-binding assay for quantitative determination of protein without interference from reducing agents or detergents. *Anal Biochem* 190: 66–70, 1990.
20. **Molitoris BA.** New insights into the cell biology of ischemic acute renal failure. *J Am Soc Nephrol* 1: 1263–1270, 1991.
21. **Molitoris BA.** Putting the actin cytoskeleton into perspective: pathophysiology of ischemic alterations. *Am J Physiol Renal Physiol* 272: F430–F433, 1997.
22. **Molitoris BA, Chan LK, Shapiro JI, Conger JD, and Falk SA.** Loss of epithelial polarity: a novel hypothesis for reduced proximal tubule Na^+ transport following ischemic injury. *J Membr Biol* 107: 119–127, 1989.
23. **Molitoris BA, Falk SA, and Dahl RH.** Ischemia-induced loss of epithelial polarity: role of tight junction. *J Clin Invest* 84: 1334–1339, 1989.
24. **Molitoris BA, Geerdes A, and McIntosh JR.** Dissociation and redistribution of Na^+,K^+-ATPase from its surface membrane actin cytoskeletal complex during cellular ATP depletion. *J Clin Invest* 88: 462–469, 1991.
25. **Morgan TE, Lockerbie RO, Minamide LS, Browning MD, and Bamburg JR.** Isolation and characterization of a regulated form of actin depolymerizing factor. *J Cell Biol* 122: 623–633, 1993.
26. **Niwa R, Nagata-Ohashi K, Takeichi M, Mizuno K, and Uemura T.** Control of actin reorganization by slingshot, a family of phosphatases that dephosphorylate ADF/cofilin. *Cell* 108: 233–246, 2002.
27. **Pfannstiel J, Cyrklaff M, Habermann A, Stoeva S, Griffiths G, Shoeman R, and Faulstich H.** Human cofilin forms oligomers exhibiting actin bundling activity. *J Biol Chem* 276: 49476–49484, 2001.
28. **Phelps PC, Smith MW, and Trump BF.** Cytosolic ionized calcium and bleb formation after acute cell injury of cultured rabbit renal tubule cells. *Lab Invest* 60: 630–642, 1989.
29. **Schwartz N, Hosford M, Sandoval RM, Wagner MC, Atkinson SJ, Bamburg JR, and Molitoris BA.** Ischemia activates actin depolymerizing factor: role in proximal tubule microvillar actin alterations. *Am J Physiol Renal Physiol* 276: F544–F551, 1999.
30. **Sutton TA and Molitoris BA.** Mechanisms of cellular injury in ischemic acute renal failure. *Semin Nephrol* 18: 490–497, 1998.
31. **Toshima J, Toshima JY, Amano T, Yang N, Narumiya S, and Mizuno K.** Cofilin phosphorylation by protein kinase testicular protein kinase 1 and its role in integrin-mediated actin reorganization and focal adhesion formation. *Mol Biol Cell* 12: 1131–1145, 2001.
32. **Vartiainen MK, Mustonen T, Mattila PK, Ojala PJ, Thesleff I, Partanen J, and Lappalainen P.** The three mouse actin-depolymerizing factor/cofilins evolved to fulfill cell-type-specific requirements for actin dynamics. *Mol Biol Cell* 13: 183–194, 2002.
33. **Venkatachalam MA, Jones DB, Rennke HG, Sandstrom D, and Patel Y.** Mechanism of proximal tubule brush border loss and regeneration following mild renal ischemia. *Lab Invest* 45: 355–365, 1981.
34. **Yang N, Higuchi O, Ohashi K, Nagata K, Wada A, Kangawa K, Nishida E, and Mizuno K.** Cofilin phosphorylation by LIM-kinase 1 and its role in Rac-mediated actin reorganization. *Nature* 393: 809–812, 1998.